Mineralogical Magazine, October 2017, Vol. 81(5), pp. 1039–1050

Leószilárdite, the first Na,Mg-containing uranyl carbonate from the Markey Mine, San Juan County, Utah, USA

Travis A. Olds[1,*], Luke R. Sadergaski[1], Jakub Plášil[2], Anthony R. Kampf[3], Peter C. Burns[1,4], Ian M. Steele[5], Joe Marty[6], Shawn M. Carlson[7] and Owen P. Mills[8]

[1] Department of Civil and Environmental Engineering and Earth Sciences, University of Notre Dame, Notre Dame, IN 46556, USA
[2] Institute of Physics, Academy of Sciences of the Czech Republic, v.v.i., Na Slovance 1999/2, 18221 Praha 8, Czech Republic
[3] Mineral Sciences Department, Natural History Museum of Los Angeles County, 900 Exposition Boulevard, Los Angeles, CA 90007, USA
[4] Department of Chemistry and Biochemistry, University of Notre Dame, Notre Dame, IN 46556, USA
[5] Notre Dame Integrated Imaging Facility, University of Notre Dame, Notre Dame, IN 46556, USA
[6] 5199 East Silver Oak Road, Salt Lake City, UT 84108, USA
[7] 245 Jule Lake Road, Crystal Falls, MI 49920, USA
[8] Applied Chemical and Morphological Analysis Laboratory, Michigan Technological University, Houghton, MI 49931, USA

[*Received 4 August 2016; Accepted 18 September 2016; Associate Editor: Stuart Mills*]

ABSTRACT

Leószilárdite (IMA2015-128), $Na_6Mg(UO_2)_2(CO_3)_6{\cdot}6H_2O$, was found in the Markey Mine, Red Canyon, White Canyon District, San Juan County, Utah, USA, in areas with abundant andersonite, natrozippeite, gypsum, anhydrite, and probable hydromagnesite along with other secondary uranium minerals bayleyite, čejkaite and johannite. The new mineral occurs as aggregates of pale yellow bladed crystals flattened on {001} and elongated along [010], individually reaching up to 0.2 mm long. More commonly it occurs as pale yellow pearlescent masses to 2 mm consisting of very small plates. Leószilárdite fluoresces green under both longwave and shortwave ultraviolet light, and is translucent with a white streak, hardness of 2 (Mohs), and brittle tenacity with uneven fracture. The new mineral is readily soluble in room temperature H_2O. Crystals have perfect cleavage along {001}, and exhibit the forms {110}, {001}, {100}, {101} and {$\bar{1}$01}. Optically, leószilárdite is biaxial (–), $\alpha = 1.504(1)$, $\beta = 1.597(1)$, $\gamma = 1.628(1)$ (white light); 2V (meas.) = 57(1)°, 2V (calc.) = 57.1°; dispersion $r > v$, slight. Pleochroism: X = colourless, Y and Z = light yellow; $X < Y \approx Z$. The average of six wavelength dispersive spectroscopic analyses provided Na_2O 14.54, MgO 3.05, UO_3 47.95, CO_2 22.13, H_2O 9.51, total 97.18 wt.%. The empirical formula is $Na_{5.60}Mg_{0.90}U_2O_{28}C_6H_{12.60}$, based on 28 O apfu. Leószilárdite is monoclinic, $C2/m$, $a = 11.6093(21)$, $b = 6.7843(13)$, $c = 15.1058(28)$ Å, $\beta = 91.378(3)°$, $V = 1189.4(4)$ Å^3 and $Z = 2$. The crystal structure ($R_1 = 0.0387$ for 1394 reflections with $I_{obs} > 4\sigma I$), consists of uranyl tricarbonate anion clusters $[(UO_2)(CO_3)_3]^{4-}$ held together in part by irregular chains of $NaO_5(H_2O)$ polyhedra sub parallel to [010]. Individual uranyl tricarbonate clusters are also linked together by three-octahedron units consisting of two Na-centred octahedra that share the opposite faces of a Mg-centred octahedron at the centre (Na–Mg–Na), and have the composition $Na_2MgO_{12}(H_2O)_4$. The name of the new mineral honours the Hungarian-American physicist, inventor and biologist Dr. Leó Szilárd (1898–1964).

Keywords: leószilárdite, new mineral, uranium, uranyl carbonate, crystal structure, Markey mine.

Introduction

Typically, uranyl carbonates are soluble ephemeral solids and are the dominant phases that precipitate

* E-mail: tolds@nd.edu
https://doi.org/10.1180/minmag.2016.080.149

from neutral to alkaline waters containing uranium (Finch and Ewing, 1992; Finch and Murakami, 1999). Uranyl carbonate complexes are exceptionally stable and dictate the mobility of uranium in carbonated groundwater, where the uranyl ion $(UO_2)^{2+}$ is readily solubilized (Langmuir 1978; Clark *et al.*, 1995; Gorman-Lewis *et al.*, 2008). With the acceptance of leószilárdite, the family of uranyl carbonate minerals now totals 34. The majority of these contain the uranyl tricarbonate complex (henceforth referred to as UTC) $[(UO_2)(CO_3)_3]^{4-}$, which is commonly present in solution coordinated with other cations (K^+, Na^+, Ca^{2+}, etc.) and the phase that ultimately precipitates is influenced by the local groundwater chemistry, pH, pCO_2 and evaporation rates (Garrels and Christ, 1959; Hostetler and Garrels, 1962). Leószilárdite differs chemically from all others as the first Na- and Mg-containing uranyl carbonate – a somewhat surprising occurrence considering the cations involved are commonly found together.

Leószilárdite is named in honour of the Hungarian-American physicist, inventor and biologist Dr. Leó Szilárd (1898–1964). Szilárd held many patents for his inventions, including those for the linear accelerator, the cyclotron, the Szilárd-Einstein refrigerator and the nuclear reactor with Enrico Fermi in 1933 – however their reactor was not based upon fission as the phenomenon had not yet been discovered. He is perhaps most well-known for envisioning the concept of, and patenting, the neutron-induced nuclear chain reaction. Likewise, he played a compelling role in the development of the United States nuclear program, by penning a letter to Franklin D. Roosevelt warning that Germany may develop nuclear weapons that harnessed the fission reaction of uranium. The famous letter, signed by Albert Einstein, jumpstarted the research and development of the Manhattan project.

The new mineral and its name were approved by the Commission on New Minerals, Nomenclature and Classification of the International Mineralogical Association (IMA2015-128). The holotype specimen is deposited in the collections of the Natural History Museum of Los Angeles County, 900 Exposition Boulevard, Los Angeles, CA 90007, USA, catalogue number 65645.

Occurrence

Leószilárdite was found underground at the Markey mine, Red Canyon, White Canyon District, San Juan County, Utah, USA (UTM coordinates; 12 S 4155830 mN, 0561730 mE, NAD27). The workings lie 1 km southwest of the Blue Lizard mine, on the east-facing side of the canyon roughly 73 km west of Blanding, Utah and 35 km south of Hite on Lake Powell. Leószilárdite was later found occurring with abundant andersonite at the Pickett Corral mine, Montrose County, Colorado, USA, but this is not considered a type locality; the description is based only on material from the Markey mine. The geology of the Markey mine is quite similar to that of the nearby Blue Lizard mine (Chenoweth, 1993) although the mineralogy of the Markey mine is notably richer in carbonate phases. As an interesting aside, this difference in mineral chemistry may be reflected by the current mine air chemistry. Preliminary underground gas measurements collected in 2016 using a hand-held Crowcon Gasman CO_2 monitor showed consistently elevated CO_2 levels at the Markey mine, averaging ~1000 ppm CO_2 with a maximum recorded value of 1600 ppm CO_2, levels considerably higher than at the nearby Blue Lizard (and Posey) mines where carbonate mineral species are less abundant.

This geological and historical information following is taken from a report by Strand (1954) contained within an application to the Defense Minerals Exploration Administration (docket 4260) for government aid to continue uranium exploration of the area surrounding the Markey mine. All large uranium deposits in the area of Red Canyon are characterized as channel-type sediments from streams that deposited the Triassic Shinarump conglomerate, and commonly cut into the underlying reddish-brown silty sandstones and mudstones of the Moenkopi Formation. Today, the characteristic red rocks of the Moenkopi Formation form much of the lower floor and walls of the canyon, assumed to be the origin of the name Red Canyon. Location and exploration of the claims encompassing the Markey mine area began in 1951 by Edward H. Eakland, Jr. and others, and the first batch of copper-uranium ore was mined and shipped to the Atomic Energy Commission mill in Monticello, Utah by the Anaconda Copper Mining Company in 1953. In total 1,214 tons of uranium ore were removed averaging 20% U_3O_8. The mine now lies abandoned and post-mining oxidation of primary minerals in the humid underground environment is responsible for producing interesting secondary uranium minerals, including abundant andersonite and natrozippeite. Leószilárdite is a relatively rare mineral in the

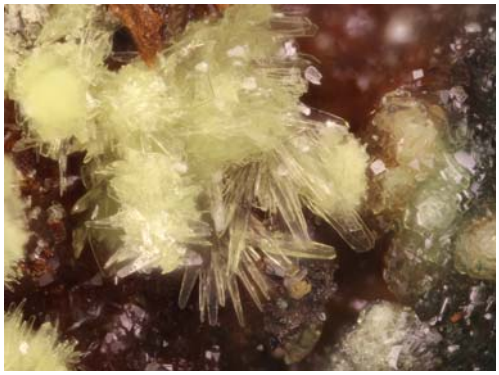

FIG. 1. Bladed pale yellow leószilárdite on andersonite. Horizontal field of view is ~1.2 mm. Travis Olds specimen and photo.

secondary carbonate assemblage at the Markey mine, and is found in areas with abundant andersonite and gypsum, along with the other secondary minerals bayleyite, čejkaite, johannite, natrozippeite and chalcanthite coating veins of uraninite in sulfide-laden carbonaceous wood fragments.

Physical and optical properties

Leószilárdite forms as aggregates of long thin pale yellow blades individually reaching 0.2 mm long, and pale yellow pearlescent masses to 2 mm composed of thin plates (Figs 1, 2 and 3). Crystals are flattened on {001} and elongated on [010], and exhibit the forms {110}, {001}, {100}, {101} and {$\bar{1}$01} (Fig. 4). No twinning was observed. Crystals are transparent with a vitreous lustre, while crystalline masses exhibit a pearly lustre. The mineral has a white streak, is weakly fluorescent green under both longwave and short-wave ultraviolet light. The Mohs hardness is ~2, estimated by the behaviour of crystals when broken. Crystals of leószilárdite are brittle with perfect {001} cleavage and even fracture. The density could not be measured due to the limited availability of material, and solubility in aqueous

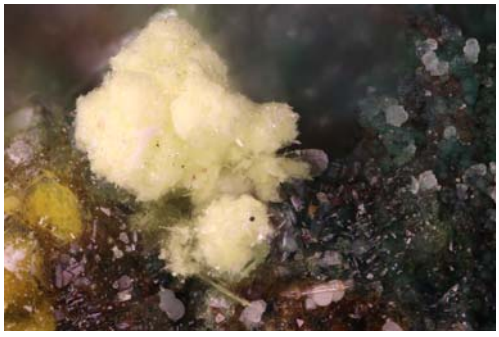

FIG. 2. Pearlescent masses of leószilárdite coat andersonite, with yellow natrozippeite and probable white spherical hydromagnesite. Horizontal field of view is ~1.9 mm. Travis Olds specimen and photo.

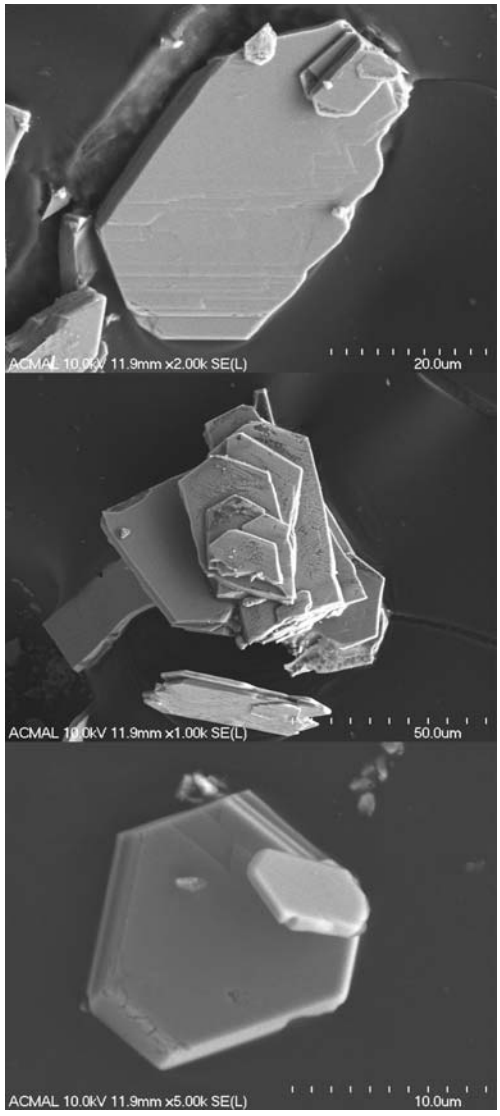

FIG. 3. Secondary electron images of leószilárdite microcrystals. Images by Owen Mills.

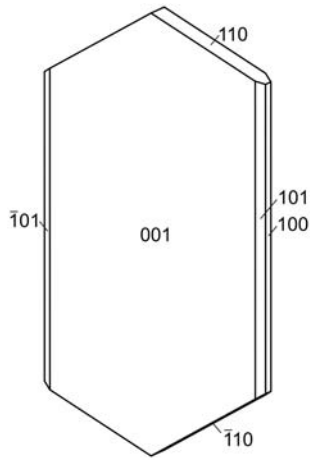

FIG. 4. Crystal drawing of leószilárdite; clinographic projection in non-standard orientation (*b* vertical).

heavy liquids. The calculated density is 3.256 g cm^{-3} based on the empirical formula.

Optically, leószilárdite is biaxial (–), with $\alpha = 1.504(1)$, $\beta = 1.597(1)$, $\gamma = 1.628(1)$ (measured in white light). The measured 2V is 57(1)°, based on extinction data collected on a spindle stage and analysed using *EXCALIBRW*; the calculated 2V is 57.1°. Dispersion is slight, $r > v$. The mineral is pleochroic with X = colourless, Y and Z = light yellow; $X < Y \approx Z$. The optical orientation is $X =$ **b**, $Y \approx$ **a**, $Z \approx$ **c**.

The Gladstone-Dale compatibility, $1 - (K_p/K_c)$, is –0.011 (superior) for the ideal formula, and –0.053 (good) for the empirical formula (Mandarino, 2007). The value for $k(UO_3) = 0.118$, given by Mandarino (1976) was used for the calculation as it yielded the best compatibilities.

Raman spectroscopy

The Raman spectrum of leószilárdite was recorded using a Bruker Instruments Sentinel-785 laser head mounted on a Nikon Optiphot-2 microscope with Peltier-cooled integrated 785 nm diode laser, operated at 200 mW, with a spot size of 100 µm and resolution of ~5 cm^{-1}. The spectrometer was calibrated with software-controlled procedures (Opus software) using neon emission lines (wavelength calibration) and Tylenol® Raman bands (frequency calibration). A background correction was applied using the Opus software.

The Raman spectrum of leószilárdite is given in Fig. 5, and the following assignments are based on those given by various authors (Čejka, 1999; Jolivet *et al.*, 1980; Urbanec and Čejka, 1979). The ν_3 $(CO_3)^{2-}$ antisymmetric stretching vibrations are observed at 1535, 1396 and 1328 cm^{-1}. No bands related to the ν_2 (δ)-bending vibration of

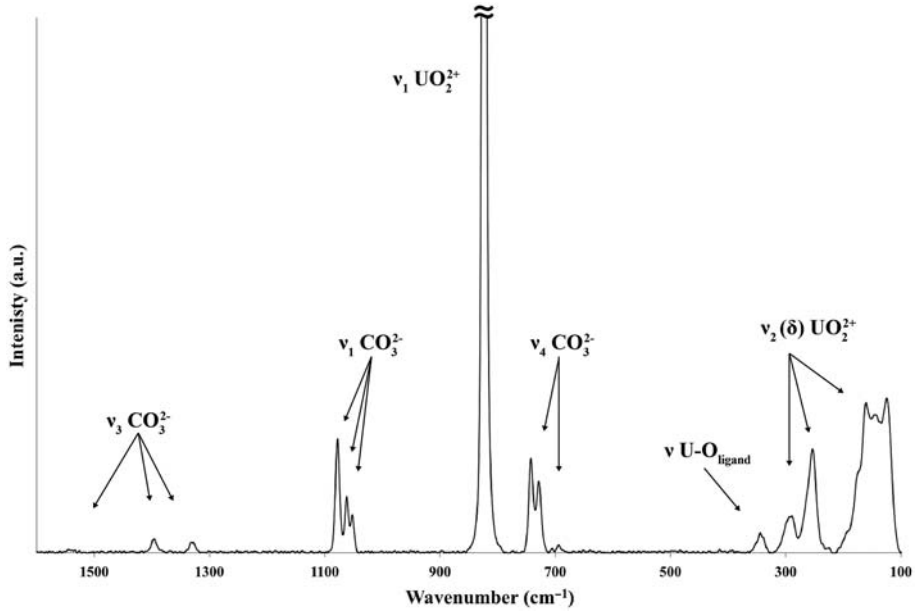

FIG. 5. The Raman spectrum of leószilárdite collected with a 785 nm laser.

TABLE 1. Chemical data for leószilárdite.

Constituent	Mean wt.%	Range	Standard. deviation	Probe standard
Na_2O	14.54	14.15–15.06	0.31	Albite
MgO	3.05	2.71–3.35	0.27	Olivine
UO_3	47.95	47.35–48.74	0.63	UO_2 (syn.)
CO_2*	22.13			
H_2O**	9.51			
Total	97.18			

*Calculated based on the structure model for 6 C per formula unit.
**Calculated to provide charge balance.

water were observed. The split ν_1 $(CO_3)^{2-}$ symmetric stretching vibrations are observed at 1078, 1062 and 1052 cm^{-1}. These three bands verify the presence of three structurally non-equivalent carbonate units seen in the X-ray data. A very strong Raman band at 824 cm^{-1} is assigned as the ν_1

TABLE 2. Powder X-ray data for leószilárdite (*d* values in Å).

I_{obs}	d_{obs}	d_{calc}	I_{calc}	*h k l*	I_{obs}	d_{obs}	d_{calc}	I_{calc}	*h k l*	I_{obs}	d_{obs}	d_{calc}	I_{calc}	*h k l*
		15.1016	4	0 0 1			2.5448	2	$\bar{2}$ 2 3			1.8204	6	0 2 7
36	**7.59**	7.5508	45	0 0 2	15	2.534	2.5403	4	$\bar{4}$ 0 3	11	1.8178	1.8128	2	3 3 3
13	5.82	5.8570	7	1 1 0			2.5366	7	$\bar{3}$ 1 4			1.8031	2	$\bar{1}$ 1 8
		5.8028	7	2 0 0			2.5233	2	0 2 4	14	1.7920	1.7985	2	3 1 7
		5.4832	25	$\bar{1}$ 1 1			2.5169	2	0 0 6			1.7958	4	$\bar{5}$ 1 5
100	**5.46**	5.4608	15	$\bar{2}$ 0 1	8	2.492	2.4880	7	4 0 3			1.7847	3	1 3 5
		5.4385	60	1 1 1			2.4845	3	3 1 4			1.7655	2	4 2 5
		5.3736	4	2 0 1			2.3277	2	$\bar{4}$ 0 4			1.7471	2	$\bar{2}$ 2 7
28	**4.64**	4.6554	24	$\bar{1}$ 1 2	8	2.317	2.3227	6	$\bar{1}$ 1 6	9	1.7444	1.7428	3	$\bar{3}$ 3 4
		4.5485	9	2 0 2			2.2891	3	2 0 6			1.7385	2	$\bar{6}$ 0 4
		3.8486	6	$\bar{2}$ 0 3			2.2557	2	0 2 5	8	1.6953	1.6961	6	0 4 0
30	**3.82**	3.8407	11	$\bar{1}$ 1 3			2.2234	4	3 1 5			1.6803	2	6 2 0
		3.7949	14	1 1 3			2.1975	4	$\bar{1}$ 3 1	9	1.6735	1.6780	2	0 0 9
		3.7754	4	0 0 4	22	2.195	2.1962	2	5 1 0			1.6737	3	$\bar{4}$ 2 6
		3.7580	3	2 0 3			2.1946	5	1 3 1			1.6686	2	$\bar{1}$ 3 6
33	**3.383**	3.3922	21	0 2 0			2.1804	3	$\bar{5}$ 1 1			1.6548	2	0 4 2
		3.3606	11	3 1 0			2.1761	4	4 2 1			1.6364	2	5 1 6
		3.2659	4	$\bar{3}$ 1 1	8	2.158	2.1574	6	0 0 7			1.6197	2	$\bar{2}$ 4 1
6	3.209	3.1910	7	$\bar{1}$ 1 4			2.1322	2	$\bar{1}$ 3 2			1.5892	2	2 4 2
		3.1304	9	2 0 4	10	2.103	2.0960	6	5 1 2	6	1.5771	1.5783	4	5 3 2
25	**3.105**	3.0943	18	0 2 2			2.0351	4	$\bar{3}$ 1 6			1.5518	3	$\bar{3}$ 3 6
		3.0467	2	3 1 2			2.0333	8	$\bar{4}$ 2 3	11	1.5482	1.5495	2	$\bar{5}$ 3 3
		2.9285	3	2 2 0			2.0299	4	$\bar{5}$ 1 3			1.5472	2	$\bar{6}$ 2 4
		2.8815	9	$\bar{2}$ 2 1	**28**	**2.0283**	2.0276	3	1 3 3			1.4913	2	2 4 4
31	**2.864**	2.8621	9	$\bar{4}$ 0 1			2.0165	3	1 1 7	5	1.4882	1.4796	2	5 3 4
		2.8367	9	4 0 1			2.0062	5	4 2 3			1.4591	2	$\bar{4}$ 4 1
		2.8131	2	0 2 3	5	1.9464	1.9523	3	3 3 0		1.4587	1.4557	3	4 4 1
		2.7684	3	3 1 3	9	1.9174	1.9244	2	$\bar{6}$ 0 1	10	1.4370	1.4375	4	$\bar{5}$ 3 5
		2.7192	7	2 2 2			1.9173	5	$\bar{1}$ 3 4					
20	2.704	2.7059	9	$\bar{2}$ 0 5	12	1.8830	1.8847	2	$\bar{6}$ 0 2					
		2.6712	10	1 1 5			1.8798	7	5 1 4					

The strongest lines are given in bold.

the $(UO_2)^{2+}$ symmetric stretching vibration. Bartlett and Cooney (1989) provide an empirical relation to derive the approximate U–O_{yl} bond length from the band position assigned to the ν_1 $(UO_2)^{2+}$ stretching vibration, which gives 1.79 Å. This value is in accordance with the U–O_{yl} bond lengths given by Burns *et al.* (1997) for the uranyl cation in hexagonal bipyramidal coordination, and the U–O_{yl} bond length of 1.79 Å derived from the X-ray data.

Raman bands at 742, 729, 705 and 695 cm^{-1} are attributed to the split doubly degenerate ν_4 (δ) $(CO_3)^{2-}$ in-plane bending vibrations. A weak band at 345 cm^{-1} is assigned as a ν (U–O_{ligand}) stretch, and the doubly degenerate ν_2 (δ) $(UO_2)^{2+}$ bending mode is found at 290 and 254 cm^{-1}, though band assignment in this region is difficult due to overlap with U–O_{ligand} stretches. Remaining bands at 193, 172, 161, 144 and 125 cm^{-1} are assigned to either ν_2 (δ) $(UO_2)^{2+}$ bending modes, U–O_{ligand} stretches, or external lattice vibration modes.

TABLE 3. Data collection and structure-refinement details for leószilárdite.

Diffractometer	Bruker Quazar II with Apex II detector
X-ray radiation/power	Mo*K*α (λ = 0.71075 Å)/50 kV, 60 mA
Temperature	298(2) K
Structural formula	$Na_6Mg(UO_2)_2(CO_3)_6{\cdot}6H_2O$
Space group	*C*2/*m*
Unit-cell dimensions	*a* = 11.6093(21) Å *b* = 6.7843(13) Å *c* = 15.1058(28) Å β = 91.378(3)°
V	1189.4(4) $Å^3$
Z	2
Density (for above formula)	3.269 g cm^{-3}
Absorption coefficient	13.862 mm^{-1}
F(000)	1044.0
Crystal size (μm)	45 × 30 × 6
θ range	1.35 to 29.26°
Index ranges	$-15 \le h \le 15$, $-8 \le k \le 8$, $-20 \le l \le 19$
Reflections collected/ unique	7517/1634; R_{int} = 0.0719
Reflections with $I_{obs} > 4\sigma(I)$	1394
Completeness to θ = 25.24°	100%
Refinement method	Full-matrix least-squares on F^2
Parameters refined	122
Goof (obs/all)	1.006/0.966
R (obs), *wR* (obs)	0.0387, 0.0847
R (all), *wR* (all)	0.0504, 0.0892
Largest diff. peak/hole	+2.34/–1.64 *e*

Chemical composition

Several crystals of leószilárdite were analysed using a Cameca SX50 electron microprobe (University of Notre Dame), operating with an accelerating voltage of 15 kV, a beam current of 10 nA and beam diameter of 25 μm. The following standards were used: Na*K*α (albite), Mg*K*α (olivine), U*M*α (synthetic UO_2). Other elements were sought but not detected. The counting time for each peak was 8 s, as was the counting time for each background. Matrix effects were accounted for using the *PAP* correction routine (Pouchou and Pichoir, 1985). The mineral contains a high proportion of volatile sodium, and the fragility of crystals under the beam led to slightly low totals (~97%) and required the analysis of multiple crystals using a wide beam. The CO_2 and H_2O contents could not be measured due to the limited amount of material available; instead they are calculated based on the structural formula with 6 C, and 28 O atoms per formula unit, and with charge balance considerations satisfied by H. Analytical data averaged for six analyses from multiple crystals are given in Table 1. The empirical formula is $Na_{5.60}Mg_{0.90}U_2O_{28}C_6H_{12.60}$. The ideal formula is $Na_6Mg(UO_2)_2(CO_3)_6{\cdot}6H_2O$, which requires Na_2O 15.88, MgO 3.45, UO_3 48.88, CO_2 22.55 and H_2O 9.24, total 100 wt.%.

Powder X-ray diffraction

Room temperature powder diffraction data (Table 2) were recorded using a Rigaku R-Axis Rapid II curved imaging plate microdiffractometer with monochromated Mo*K*α radiation. A Gandolfi-like motion on the φ and ω axes was used to randomize diffraction from the sample. Observed *d*-values and intensities were derived by profile fitting using *JADE 2010* software (Materials Data, Inc.). Unit-cell parameters refined from the powder data are as follows: *a* = 11.588(6) Å, *b* = 6.767(6) Å, *c* = 15.081(6) Å, β = 91.453(9)°, V = 1182.2(13) $Å^3$.

Single-crystal X-ray diffraction

Single crystal data were collected from an optically homogeneous bladed crystal using Mo*K*α X-rays from a microfocus source and an Apex II CCD-based detector mounted to a Bruker Apex II Quazar

TABLE 4. Atomic coordinates and displacement parameters (Å^2) for leószilárdite.

Atoms	x	y	z	$U_{eq/iso}$	U^{11}	U^{22}	U^{33}	U^{23}	U^{13}	U^{12}
U1	0.312623(3)	0.5	0.72748(2)	0.01418(13)	0.0113(2)	0.0176(2)	0.0137(2)	0	0.00213(13)	0
Na1	0.3146(4)	0	0.83965(29)	0.0220(6)	0.0188(14)	0.0249(17)	0.0223(18)	0	0.0011(13)	0
Na2	0.4274(2)	0.2611(5)	0.3783(2)	0.0274(7)	0.0298(18)	0.0259(17)	0.0267(17)	–0.0019(12)	0.0042(13)	–0.0032(13)
Mg1	0.5	0	1	0.0163(9)	0.0128(19)	0.0216(25)	0.0146(17)	0	0.0050(14)	0
C1	0.6045(10)	0	0.8216(7)	0.0199(20)	0.0189(19)	0.032(6)	0.0093(23)	0	0.0015(19)	0
C2	0.3150(9)	0.5	0.5369(7)	0.0202(14)	0.016(3)	0.029(4)	0.0165(14)	0	–0.0008(18)	0
C3	0.0336(10)	0	0.8234(7)	0.0201(20)	0.0177(18)	0.028(6)	0.014(3)	0	0.0003(20)	0
O1	0.6033(6)	0	0.7349(4)	0.0142(14)	0.017(4)	0.017(4)	0.008(2)	0	0.002(2)	0
O2	0.0303(6)	0	0.7359(5)	0.0149(14)	0.019(4)	0.013(3)	0.0129	0	–0.002(2)	0
O3	–0.0659(6)	0	0.8611(5)	0.0201(15)	0.016(2)	0.027(4)	0.017(3)	0	0.001(2)	0
O4	0.4069(6)	0.5	0.5869(5)	0.0225(12)	0.014(3)	0.038(4)	0.0158(19)	0	0.0022(16)	0.0225(12)
O5	0.2193(6)	0.5	0.5825(5)	0.0205(12)	0.014(2)	0.031(3)	0.017(2)	0	–0.001(2)	0
O6	0.3153(7)	0.5	0.4549(5)	0.0243(12)	0.019(4)	0.038(4)	0.0155(14)	0	0.0002(20)	0
O7	0.3151(5)	0.2359(9)	0.7269(3)	0.0237(10)	0.030(3)	0.0208(16)	0.0196(21)	–0.001(1)	–0.0036(17)	–0.001(2)
O8	0.5152(7)	0	0.8644(5)	0.0221(14)	0.0183(16)	0.036(4)	0.0124(20)	0	0.0029(16)	0
O9	0.7062(7)	0	0.8605(5)	0.0345(22)	0.0179(20)	0.075(7)	0.010(3)	0	0.001(2)	0
O10	0.1271(7)	0	0.8665(5)	0.0401(22)	0.0173(16)	0.089(7)	0.014(3)	0	–0.0004(17)	0
Ow1	0.5647(7)	0	0.4168(6)	0.0293(16)	0.020(4)	0.037(4)	0.030(5)	0	0.002(3)	0
Ow2	0.6259(6)	0.2133(12)	1.0210(4)	0.0493(21)	0.041(3)	0.078(5)	0.029(3)	–0.025(3)	0.0176(23)	–0.042(3)

TABLE 5. Selected bond distances in leószilárdite.

U1–O7 (×2)	1.792(6)	Na2–O1	2.482(6)
U1–O1	2.477(7)	Na2–O2	2.426(6)
U1–O2	2.486(7)	Na2–O4	2.560(7)
U1–O3	2.410(7)	Na2–O5	2.537(6)
U1–O4	2.392(7)	Na2–O6	2.394(7)
U1–O5	2.438(7)	Na2–Ow1	2.444(7)
U1–O9	2.407(8)	<Na2–O>	2.47
<U1–O_{Ur}>	1.792		
<U1–O_{Eq}>	2.429		
Mg1–O8 (×2)	2.061(7)	C1–O1	1.309(12)
Mg1–Ow2 (×4)	2.075(6)	C1–O8	1.235(13)
<Mg1–O>	2.070	C1–O9	1.307(14)
		<C1–O>	1.28
Na1–O10	2.223(9)	C2–O4	1.293(13)
Na1–O7 (×2)	2.337(6)	C2–O5	1.322(13)
Na1–O8	2.350(9)	C2–O6	1.239(13)
Na1–Ow2 (×2)	2.633(9)	<C2–O>	1.28
<Na1–O>	2.32		
		C3–O2	1.321(12)
		C3–O3	1.300(13)
		C3–O10	1.253(13)
		<C3–O>	1.29

three-circle diffractometer. Reflections were integrated and corrected for Lorentz, polarization and background effects using the Bruker program *SAINT*. A multi-scan semi-empirical absorption correction was applied using equivalent reflections in *SADABS-2012*. An initial structure model was obtained by the charge-flipping method using *SHELXT* (Sheldrick, 2015) in the space group *C*2/*m*. Refinement proceeded by full-matrix least-squares on F^2 using *SHELX-2013* (Sheldrick, 2008), and refined to an R_1 of 3.87% for 1394 reflections with $I_{obs} > 4\sigma(I)$. Rigid bond restraints were applied to the anharmonic displacement parameters of all atoms using the *DELU* and *RIGU* instructions in *SHELXL*. Hydrogen atom positions were sought but were not located in difference-Fourier maps, as a result the nature of H-bonding interactions is not discussed. Further details regarding the data collection and refinement are given in Table 3. Final atom coordinates and displacement parameters are listed in Table 4, selected interatomic distances in Table 5, and the bond-valence sums are given in Table 6. The original crystallographic information file (cif) has been deposited with the Principal Editor of Mineralogical Magazine and is available from http://www.minersoc.org/pages/e_journals/dep_mat_mm.html

Features of the crystal structure

In the structure of leószilárdite there is one independent U, three C, one Mg, two Na and 12 O sites ($Z = 2$). It contains hexagonal uranyl bipyramids chelated by three CO_3 groups, and has a cluster topology based upon uranyl tricarbonate anions (UTC) of the formula $[(UO_2)(CO_3)_3]^{4-}$ (Burns, 2005). Leószilárdite is a member of the uranyl tricarbonates, Strunz class 05.ED, with UO_2:$CO_3 = 1:3$. It bears most resemblance to čejkaite (Plášil *et al.*, 2013), synthetic $Na_4(UO_2)(CO_3)_3$ (Li *et al.*, 2001; Císařová *et al.*, 2001) and ježekite (Plášil *et al.*, 2015) in that the structures of all of these phases contain chains of face-sharing sodium polyhedra linked to the uranyl tricarbonate clusters. However, the structure of leószilárdite is unique amongst the uranyl carbonates with respect to the arrangement of Na^+ and Mg^{2+} cations, and represents the first natural uranyl carbonate containing both Na and Mg as essential constituents.

The uranyl hexagonal bipyramid shares two edges with face-sharing chains of $Na(H_2O)O_5$ trigonal prisms (Na2) that extend along [010] (Fig. 6). The structure also contains a distinctive three-octahedron unit of the formula $Na_2MgO_{12}(H_2O)_4$ consisting of two Na-centred octahedra that share the opposite faces of a Mg-

TABLE 6. Bond-valence sums for leószilárdite.*

Atom	O1	O2	O3	O4	O5	O6	O7	O8	O9	O10	Ow1	Ow2	Σ_{cat}
U1	0.44	0.43	0.50	0.52	0.47		1.65 × 2→		0.50				6.16
Na1							0.21 × 2→	0.20		0.28		0.09 × 2→	1.08
Na2	0.14 × 2↓	0.16 × 2↓		0.11 × 2↓	0.12 × 2↓	0.18 × 2↓					0.16 × 2↓		0.87
Mg1								0.37 × 2→				0.36 × 4→	2.16
C1	1.25							1.52	1.25				4.02
C2				1.30	1.20	1.50							4.01
C3		1.20	1.28							1.45			3.93
Σ_{an}	2.00	2.01	1.77	2.08	2.03	1.91	1.88	2.12	1.75	1.77	0.35	0.46	

*Multiplicities indicated by × 2→, × 2↓ or × 4→; Na^{+}–O from Wood and Palenik (1999); Mg^{2+}–O and C^{4+}–O bond strengths taken from Brown and Altermatt (1985); U^{6+}–O bond strength from Burns *et al.* (1997).

centred octahedron at the centre (Na1–Mg1–Na1). These three-octahedron units, aligned along [101], further connect the UTC units (Fig 7).

Chains of Na-centred polyhedra found in čejkaite coordinate to UTC units by sharing only apices with carbonate triangles from six individual uranyl polyhedra. In contrast, each Na-centred polyhedron in the chains of ježekite shares one edge with a uranyl polyhedron and one apex with the carbonate triangle of a different UTC unit. Individual Na-centred octahedra in the chains of leószilárdite coordinate to three UTC units, sharing two edges of uranyl polyhedra and one apex of a CO_3 triangle, each (Fig. 8). The structural formula obtained from the X-ray data is $Na_6Mg(UO_2)_2(CO_3)_6{\cdot}6H_2O$, $Z = 2$, with $D_{calc} = 3.269$ g cm^3.

Hazen *et al.* (2016) predicted 16 yet undiscovered UTC minerals on the basis of isomorphous substitutions of some elements common to natural groundwater into known structures. They also predict 11 other UTC phases, bearing similar compositions or structures to known synthetic phases. Leószilárdite was not amongst the predicted phases, but highlights an unfortunate downside to estimations like these; in that our inability to predict novel arrangements of cation polyhedra in uranyl carbonate minerals prevents us from fully understanding these systems. Many of our recent descriptions of uranyl carbonates from Red Canyon, Utah, USA and Jáchymov, Czech Republic bear little to no resemblance to the sensible chemical substitutions expected in natural minerals, nor to any synthetic phases not yet found to occur naturally. Rather, nearly all recent new uranyl carbonate minerals constitute novel topological arrangements; in addition to a unique class of hybrid uranyl carbonate cluster minerals that contain bridging uranyl pentagonal bipyramid clusters. We are in the process of describing two such minerals; the first includes a combination of uranyl tricarbonate (UTC) and dicarbonate units, which share apices with trimeric $[(UO_2)_3O(OH)_3]^{+}$ cluster units in ewingite (IMA2016-012). The second is an unnamed Ca, UTC mineral found by one of the authors (J.M.) in the Markey Mine, and includes UTC-bridged monomeric UO_7 units. Several uranyl carbonate minerals containing uranyl pentagonal bipyramids arranged into sheets are known; including fontanite (Hughes and Burns, 2003), wyartite (Burns and Finch, 1999), bijvoetite-Y (Li and Burns, 2001) and roubaultite (Ginderow and Cesbron, 1985). However, the structures of ewingite and the unnamed Markey mine phase are unique as the

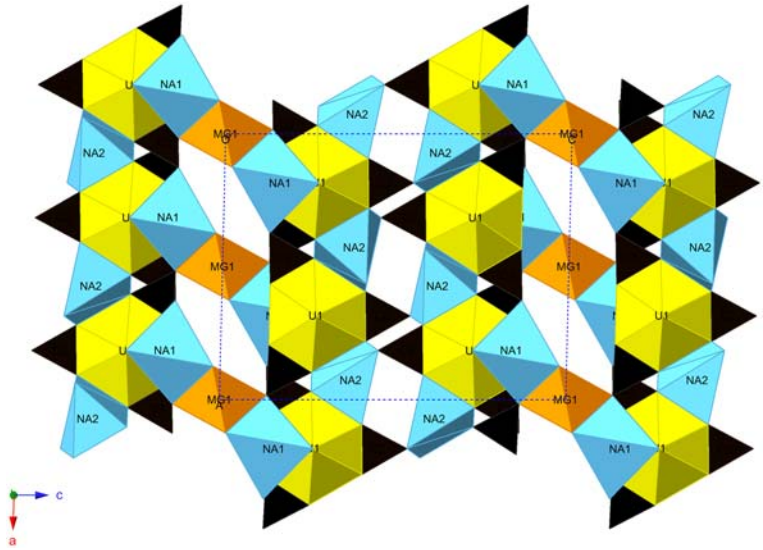

FIG. 6. A polyhedral representation of the structure of leószilárdite down *b*. The unit cell is shown as dashed lines.

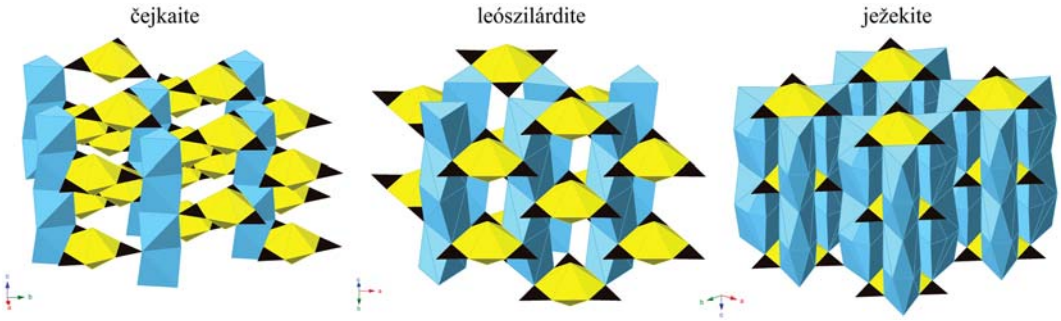

FIG. 7. Irregular chains of Na-polyhedra display varying degrees of coordination to UTC units in the related minerals čejkaite, leószilárdite and ježekite. Uranium (yellow), sodium (blue), carbon (black). Various cations have been omitted to highlight the chains of Na-polyhedra in each structure.

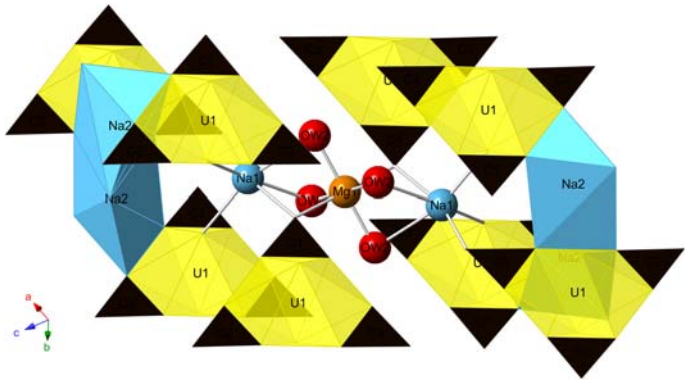

FIG. 8. The coordination environment about three-octahedron Na1–Mg1–Na1 units in the structure of leószilárdite, and their connectivity to uranyl and carbonate oxygen atoms.

first cluster, and open sheet topologies to contain this combination, respectively.

The rarity of leószilárdite is due mostly to the ephemeral nature of the mineral, and it may be a more common constituent in uranyl carbonate assemblages where the rate of dissolution is slow, and Na^{+} and Mg^{2+} are available. Newly described uranyl carbonate mineral structures motivate our work while supplementing our observations of the chemistry of uranium in carbonated groundwater. The search for rare uranyl carbonate structures continues, as it aids in delineating the complicated series of dissolution and precipitation reactions that these minerals are involved in.

Acknowledgements

Support for this work is provided by the Chemical Sciences, Geosciences and Biosciences Division, Office of Basic Energy Sciences, Office of Science, U.S. Department of Energy, Grant No. DE-FG02-07ER15880. We thank the ND Energy Materials Characterization Facility for the use of the single-crystal X-ray diffraction and Raman spectroscopy instruments. A portion of this study was funded by the John Jago Trelawney Endowment to the Mineral Sciences Department of the Natural History Museum of Los Angeles County. Jakub Plášil is thankful for the support from the project No. LO1603 under the Ministry of Education, Youth and Sports National sustainability programme I of Czech Republic.

References

Bartlett, J.R. and Cooney, R.P. (1989) On the determination of uranium-oxygen bond lengths in dioxouranium(VI) compounds by Raman spectroscopy. *Journal of Molecular Structure*, **193**, 295–300.

Brown, I.D and Altermatt, D. (1985) Bond-valence parameters obtained from a systematic analysis of the inorganic crystal structure database. *Acta Crystallographica,* **B41**, 244–248.

Burns, P.C. (2005) U^{6+} minerals and inorganic compounds: insights into an expanded structural hierarchy of crystal structures. *The Canadian Mineralogist*, **43**, 1839–1894.

Burns, P.C. and Finch, R.J. (1999) Wyartite: Crystallographic evidence for the first pentavalent-uranium mineral. *American Mineralogist*, **84**, 1456–1460.

Burns, P.C., Ewing, R.C. and Hawthorne, F.C. (1997) The crystal chemistry of hexavalent uranium: polyhedron geometries, bond-valence parameters, and polymerization of polyhedra. *The Canadian Mineralogist*, **35**, 1551–1570.

Čejka, J. (1999) Infrared spectroscopy and thermal analysis of the uranyl minerals. Pp. 521–622 in: *Uranium: Mineralogy, Geochemistry and the Environment* (P.C. Burns and R.C. Ewing, editors). Reviews in Mineralogy, 38. Mineralogical Society of America, Washington DC.

Chenoweth, W.L. (1993) The Geology and Production History of the Uranium Deposits in the White Canyon Mining District, San Juan County, Utah. *Utah Geological Survey Miscellaneous Publication*, **93–3**, 26 pp.

Císařová, I., Skála, R., Ondruš, P. and Drábek, M. (2001) Trigonal $Na_4[UO_2(CO_3)_3]$. *Acta Crystallographica*, **E57**, i32–i34.

Clark, D.L., Hobart, D.E. and Neu, M.P. (1995) Actinide carbonate complexes and their importance in actinide environmental chemistry. *Chemical Reviews*, **95**, 25–48.

Finch, R.J. and Ewing, R.C. (1992) The corrosion of uraninite under oxidizing conditions. *Journal of Nuclear Materials*, **190**, 133–156.

Finch, R.J. and Murakami, T. (1999) Systematics and paragenesis of uranium minerals. Pp. 91–179 in: *Uranium: Mineralogy, Geochemistry and the Environment* (P.C. Burns and R.C. Ewing, editors). Reviews in Mineralogy, **38**. Mineralogical Society of America, Washington DC.

Garrels, R.M. and Christ, C.L. (1959) Behavior of uranium minerals during oxidation. Pp. 81–89 in: *Geochemistry and Mineralogy of the Colorado Plateau Uranium Ores* (R.M. Garrels, R.M. and E.S. Larsen, editors). United States Geological Survey Professional Paper, **320**.

Ginderow, D. and Cesbron, F. (1985) Structure de la roubaultite, $Cu_2(UO_2)_3(CO_3)_2O_2(OH)_2(H_2O)_4$. *Acta Crystallographica,* **C41**, 645–657.

Gorman-Lewis, D., Burns, P.C. and Fein, J.B. (2008) Review of uranyl mineral solubility measurements. *Journal of Chemical Thermodynamics*, **40**, 335–352.

Hazen, R.M., Hummer, D.R., Hystad, G., Downs, R.T. and Golden, J.J. (2016) Carbon mineral ecology: Predicting the undiscovered minerals of carbon. *American Mineralogist*, **101**, 889–908.

Hostetler, P.B. and Garrels, R.M. (1962) Transportation and precipitation of uranium and vanadium at low temperatures, with special reference to sandstone-type uranium deposits. *Economic Geology*, **57**, 137–167.

Hughes, K.A. and Burns, P.C. (2003) A new uranyl carbonate sheet in the crystal structure of fontanite, $Ca[(UO_2)_3(CO_3)_2O_2](H_2O)_6$. *American Mineralogist*, **88**, 962–966.

Jolivet, J.P., Thomas, Y. and Taravel, B. (1980) Vibrational study of coordinated CO_3^{2-} ions. *Journal of Molecular Structure*, **60**, 93–98.

Langmuir, D. (1978) Uranium solution-mineral equilibria at low temperatures with applications to sedimentary

ore deposits. *Geochimica Cosmochima Acta*, **42**, 547–569.

Li, Y. and Burns, P.C. (2001) A new rare-earth-element uranyl carbonate sheet in the structure of bijvoetite. *The Canadian Mineralogist*, **37**, 153–162.

Li, Y., Krivovichev, S.V. and Burns, P.C. (2001) The crystal structure of $Na_4(UO_2)(CO_3)_3$ and its relationship to schröckingerite. *Mineralogical Magazine*, **65**, 297–304.

Mandarino, J.A. (1976) The Gladstone-Dale relationship – Part 1: derivation of new constants. *The Canadian Mineralogist*, **14**, 498–502.

Mandarino, J.A. (2007) The Gladstone–Dale compatibility of minerals and its use in selecting mineral species for further study. *The Canadian Mineralogist*, **45**, 1307–1324.

Plášil, J., Fejfarová, K., Dušek, M., Škoda, R. and Rohlíček, J. (2013) Revision of the symmetry and the crystal structure of čejkaite, $Na_4(UO_2)(CO_3)_3$. *American Mineralogist*, **98**, 549–553.

Plášil, J., Hloušek, J., Kasatkin, A.V., Belakovskyi, D.I., Čejka, J. and Chernyshov, D. (2015) Ježekite, $Na_8[(UO_2)(CO_3)_3](SO_4)_2{\cdot}3H_2O$, a new uranyl mineral from Jáchymov, Czech Republic. *Journal of Geosciences*, **60**, 259–267.

Pouchou, J.L. and Pichoir, F. (1985) "PAP" (φρZ) procedure for improved quantitative microanalysis. Pp. 104–160 in: *Microbeam Analysis* (J.T. Armstrong, editor). San Francisco Press, San Francisco, USA

Sheldrick, G.M. (2008) A short history of SHELX. *Acta Crystallographica*, **A64**, 112–122.

Sheldrick, G.M. (2015) SHELXT – Integrated space-group and crystal-structure determination. *Acta Crystallographica*, **A71**, 3–8.

Strand, E. (1954) *Report on the North Markey Group Red Canyon District*, DMEA docket 4260: Defense Minerals Exploration Administration (DMEA) dockets, available online: http://minerals.usgs.gov/dockets/ut.htm

Urbanec, Z. and Čejka, J. (1979) Infrared spectra of rutherfordine and sharpite. *Collection of Czechoslovak Chemical Communications*, **44**, 1–9.

Wood, R.M. and Palenik, G.J. (1999) Bond valence sums in coordination chemistry. Sodium-oxygen complexes. *Inorganic Chemistry*, **38**, 3926–3930.